JOURNAL OF CATALYSIS 125, 67–76 (1990)

Structure and Reactivity of Ammonia Synthesis Catalysts Derived from $CeRu_2$ Precursors: A Study by *in Situ* X-Ray Absorption Spectroscopy

ANDREW P. WALKER,* TREVOR RAYMENT,* RICHARD M. LAMBERT,*,[1] AND RICHARD J. OLDMAN†

*Department of Chemistry, University of Cambridge, Cambridge CB2 1EW, England; and †I. C. I. Chemicals & Polymers, Research and Technology, P.O. Box 8, The Heath, Runcorn, Cheshire WA7 4QE, England

Received October 2, 1989; revised March 21, 1990

The activation, steady-state performance, and poisoning of efficient ammonia synthesis catalysts derived from a $CeRu_2$ precursor have been studied by *in situ* X-ray absorption spectroscopy at 50 bar pressure and at temperatures up to 450°C. The EXAFS and near-edge data *supported by earlier XRD studies under identical conditions* indicate that the active phase consists of ultradispersed, electron-rich Ru entities with low metal–metal coordination and in intimate contact with the CeH_{2+x} support. Oxidation of this material yields CeO_2/Ru; this system is catalytically inert and exhibits none of the unusual structural or electronic properties of the active CeH_{2+x}/Ru catalyst.

INTRODUCTION

Catalysts derived from rare earth intermetallic precursors can exhibit very high specific activities for ammonia synthesis; in some cases the reported performance exceeds that of the well-established Fe-based industrial catalyst by as much as an order of magnitude (*1*). X-ray diffraction (XRD) methods have been used to examine catalysts of this type after use (*1, 2*), although such postmortem measurements are of limited value due to the extreme air sensitivity of these materials. In an earlier paper (*3*) we reported on the results of a controlled atmosphere *in situ* XRD study of the genesis and reactive behaviour of ammonia synthesis catalysts derived from $CeRu_2$, $CeCo_2$, and $CeFe_2$; these observations were coupled with concurrent measurements of the catalytic activity. It was found that $CeRu_2$ activated by exposure to N_2/H_2 generated the most active catalysts and that these materials consisted of Ru metal in contact with a cerium hydride support. When the hydride-based catalyst was converted to the corresponding oxide-based material by *in situ* oxidation, it was found that there was no significant change in size of the XRD-visible Ru particles (~35 Å)—*although the catalytic activity was completely suppressed.* The inference would appear to be that the active, hydride-based catalyst must contain a large amount of a highly active form of Ru which is undetectable by XRD.

In this paper we describe the results of an *in situ* study by X-ray absorption spectroscopy (XAS) in which both EXAFS and near-edge data were obtained from the chemically evolving systems which are generated by exposure of a $CeRu_2$ precursor to various reactive atmospheres at pressures of 50 bar and at temperatures up to 450°C. A particular feature of the work is that measurements of ammonia synthesis activity or other significant changes could be made under the relevant conditions of temperature and pressure, while the sample was actually in the

[1] To whom correspondence should be addressed.

0021-9517/90 $3.00

synchrotron beam. The principal object of the work is to characterise further the active catalyst phase which evaded direct observation in our earlier XRD investigation. Here, EXAFS and near-edge data, *supported by the earlier XRD results,* indicate that the catalytically active system CeH_{2+x}/Ru contains ultradispersed Ru entities in which the metal–metal coordination is unusually low; it is also possible that these species are electron rich compared to ordinary Ru metal. The ostensibly similar but inactive system CeO_2/Ru does not exhibit these properties.

EXPERIMENTAL

The controlled atmosphere cell used for *in situ* XAS measurements was a modified version of the device used in our earlier *in situ* XRD investigation of ammonia synthesis over cerium–transition metal systems (*3*). This cell has been described in detail elsewhere (*4*); it was adapted to permit the detection of the fluorescent X rays for the present work and could be operated at 50 bar and 450°C whilst in the synchrotron beam. *Thus the present XAS observations and our earlier XRD measurements* (*3*) *employed identical sample environments.*

The nature of the measurements necessitated working in the fluorescence mode rather than in the more commonly used transmission mode. Within these materials, the attenuation length (~20 μm) at photon energies just above the absorption edge would require the preparation of very thin pinhole-free samples if transmission geometry were to be employed. This would be very difficult, especially in view of the air-sensitive nature of the $CeRu_2$ precursor. In addition, the fragmentation of starting material which inevitably occurs during sample activation would totally preclude the use of the transmission mode. Furthermore, in the fluorescence mode, the effective penetration depth for shallow angles of photon incidence is ~3.4 μm. This is close to the penetration depth (~2.5 μm) of the X rays employed in our earlier XRD study of these materials so that the present XAS results may be usefully compared with the earlier XRD data.

Intermetallic samples were prepared by electron beam melting of the constituent metals under high vacuum followed by annealing at 500°C for 1 month in an evacuated quartz ampoule. For each run a catalyst charge of approximately 0.3 g was crushed to a particle size of 50–250 μm and loaded into the sample cell under an argon atmosphere. The cell was then sealed and transferred to the spectrometer. In our earlier work (*3*) XRD observations indicated that such controlled atmosphere sample-handling techniques resulted in no detectable oxidation of the fresh catalyst charge: the initial XAS measurement on the intermetallic precursor confirmed this.

Reactant gases (BOC Ltd.) were used without additional purification: premixed CO/H_2 (33/67; impurities: O_2 5 ppm, H_2O 2 ppm, and CO_2 20 ppm) and premixed N_2/H_2 (25/75; impurities: O_2 4 ppm and H_2O 4 ppm). A flow rate of 20 standard cm^3 per minute (sccm) was used with total gas pressures of between 1 and 50 bar. Production of ammonia was monitored using a titration technique, after absorption of the product in the effluent stream by 0.1 *M* sulfuric acid solution. Calibration tests using inlet streams of up to 10% ammonia in nitrogen revealed that all the ammonia was absorbed by the acid under these conditions.

The Ru *K*-edge XA spectra were collected over the range 21,800–22,800 eV in the fluorescence mode; measurements were made at SERC Daresbury Laboratory on station 9.2. A Si(220) double crystal, order-sorting monochromator was used, operating at a resolution of 4 eV. Incident intensity (I_0) was measured by an ionisation chamber, while fluorescent intensity (I_F) was recorded using a set of 13 solid-state energy dispersive detectors (Canberra). Each detector was windowed around the Ru$K\alpha$ fluorescence energy to maximise the signal-to-background ratio. Several spectra were taken of the catalyst under each condition, both to check reproducibility and to allow improvement of the signal-to-noise ratio by addition of the spectra; each scan took ~30 min. Measurements on the activated catalysts were made initially at 450°C (reaction temperature) and then at room temperature—the latter in an attempt to reduce thermal smearing of the EXAFS data.

Quantification of the EXAFS data by modeling to match theoretical and experimental data was carried out using program EXCURVE at Daresbury Laboratory (*5*). With this program the EXAFS data are Fourier filtered and subsequently modeled using a least-squares fitting routine and calculated phase shifts which had previously been refined in the same program against data for standard materials (e.g., Ru powder). The quality of the data was such that only the first metal–metal coordination shell could be successfully modeled.

Measurements were made at shallow angles of X-ray incidence to facilitate *in situ* studies of the catalyst bed and to probe selectively the outer surface of the catalyst particles. This calls for appropriate allowances to be made during quantification of the EXAFS data. In conventional 45°/45° geometry (*6*) I_F/I_0 is linearly dependent on the absorption coefficient for dilute samples or thin layers. Departure from these conditions leads effectively to a reduction in the normalised EXAFS amplitudes and uncertainty in the evaluation of coordination numbers. However, since the average absorption coefficient varies relatively slowly at wavelengths beyond the absorption edge, it is possible to make a reasonable assessment of correction factors for the coordination numbers, knowing angle of incidence and sample thickness. In the present case, using program ABSCAL (*7*), it has been shown that at angles of incidence of 1° XAS probes the outermost few microns of the catalyst particles and that normalised EXAFS amplitudes are reduced to ~0.36 of their ideal values. Since we are dealing with a concentrated species and relatively large catalyst granules, the results are insensitive to small variations in angle of incidence in the range 0.3–3.0°. Program ABSCAL is based on ideas originally presented in Ref. (*6*) and more recently developed to consider films (*8*). In our case coordination numbers derived by modeling to match theoretical and experimental data should therefore be multiplied by a factor of ~2.8.

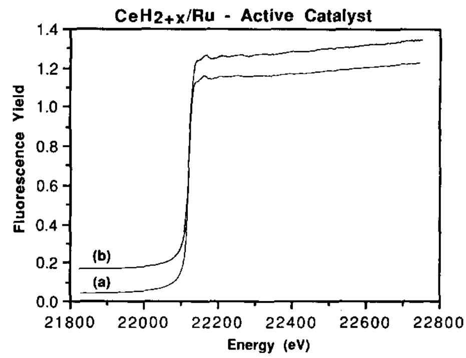

FIG. 1. XAS traces of the active catalyst CeH_{2+x}/Ru at (a) 450°C and (b) room temperature.

RESULTS

The $CeRu_2$ was first characterised in 2 bar N_2/H_2 (1/3) at room temperature; under these conditions the intermetallic is completely unreactive (*3*). After recording two spectra the gas pressure was raised to 50 bar and the temperature increased to 450°C. XAS data obtained by the addition of five consecutive spectra under these conditions are shown in Fig. 1. The *concurrently measured* ammonia synthesis activity of this catalyst at 450°C is shown in Fig. 2. It can be seen that the activity rose rapidly, achieving a steady rate of ammonia production after approximately 1 h. The catalyst was then cooled to room temperature, and further XA spectra were recorded: Figure 1 also shows the room temperature spectrum of the active phase obtained by the addition of two consecutive XAS traces. As expected, the EXAFS oscillations can be seen more clearly in the room temperature spectrum, due to the reduced smearing from the Debye–Waller factor. The k^3-weighted data fit of the catalyst at room temperature is shown

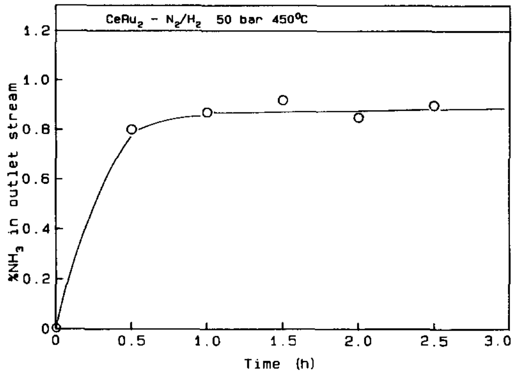

FIG. 2. Ammonia synthesis activity data for N_2/H_2 activation of the $CeRu_2$ precursor alloy at 50 bar and 450°C. These data were collected while the XAS traces of Fig. 1a were being recorded.

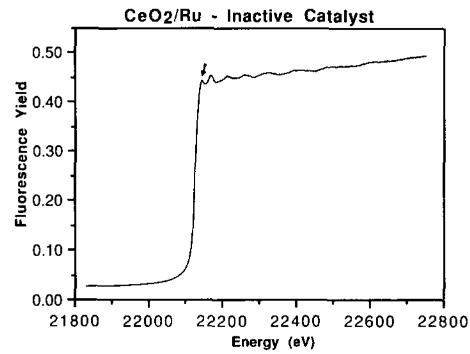

FIG. 4. XAS trace of the inactive CeO_2/Ru catalyst at room temperature. The important near-edge feature is arrowed.

in Fig. 3; this yields a Ru–Ru nearest neighbour distance of 2.66 Å, with a Ru–Ru coordination number of 5.3.

Our earlier *in situ* XRD reaction data (*3*) revealed that the catalytic activity of these cerium/transition metal-derived systems was entirely quenched by treating the active catalyst in a CO/H_2 mixture at 450°C. XRD analysis showed that the active cerium hydride/transition metal system was converted to an inactive cerium oxide/transition metal system under these conditions. The origin of this drastic change in behaviour was not revealed by the XRD measurements, so the phenomenon was investigated

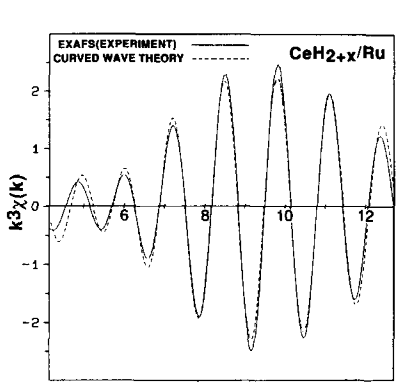

FIG. 3. Data fit of $k^3\chi(k)$ against k for the active CeH_{2+x}/Ru catalyst at room temperature.

by XAS as follows. After the room temperature X-ray absorption spectrum of the active catalyst had been recorded, the temperature was increased to 450°C *in 50 bar of CO/* H_2. After 1 h under these conditions, during which time a spectrum was recorded, the temperature was lowered to room temperature and two further spectra were obtained: the trace resulting from addition of these two room temperature spectra is shown in Fig. 4. A comparison of Figs. 1 and 4 reveals significant differences between the two systems. First of all, the magnitude of the EXAFS is much greater in the inactive CeO_2/Ru catalyst. Secondly, the edge feature (arrowed) in Fig. 4 is not present in the spectrum of the active CeH_{2+x}/Ru system.

The k^3-weighted data fit of the CeO_2/Ru catalyst at room temperature is shown in Fig. 5. This analysis yields a Ru–Ru first shell distance of 2.63 Å, and a Ru–Ru coordination number of 10.4. After the room temperature CeO_2/Ru spectra had been recorded, the gas feed was switched to 50 bar of N_2/H_2, and the catalyst temperature increased to 450°C. The XAS traces recorded during this high-temperature period were identical to those obtained at the same temperature in the CO/H_2 atmosphere. Furthermore, no ammonia synthesis activity could be detected with this system, in agreement with the results from our earlier XRD/reaction study of this catalyst (*3*).

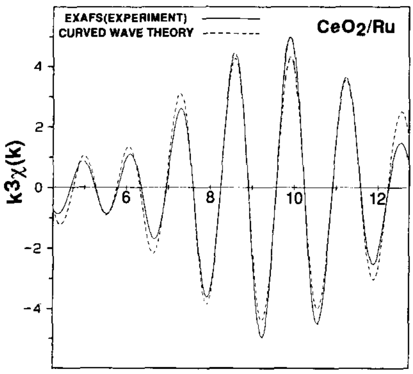

FIG. 5. Data fit of $k^3\chi(k)$ against k for the inactive CeO_2/Ru catalyst at room temperature.

In their work on Cu/rare earth oxide methanol synthesis catalysts derived from Cu/rare earth intermetallics (*4*), Nix *et al.* found that superior catalytic activity could be induced by preforming the metal hydride before treatment with CO/H_2. Therefore in the present case, to investigate what effect, if any, preforming the binary rare earth hydride had on the ultimate oxide/ruthenium system, an additional experiment was performed. A fresh charge of the $CeRu_2$ precursor alloy was loaded into the cell and subsequently treated in 50 bar CO/H_2 at 450°C for several hours, thus bypassing the cerium hydride stage. The XA spectra recorded during this period showed that the ruthenium particles generated by this treatment had a morphology identical to that of those produced by the oxidation of the CeH_{2+x}/Ru active catalyst. Following the treatment, the gas feed was switched to the N_2/H_2 mixture, while the catalyst temperature was held constant at 450°C. Again, no changes in the XA spectra were observed, and no ammonia synthesis activity was detected.

DISCUSSION

The XAS data presented in Figs. 1 and 4 clearly show that the ruthenium environment is very different in the two catalyst systems studied here. Within the experimental error and taking into account estimated uncertainties in the fitting procedure, we find that the measured Ru–Ru bond distances are the same in both catalysts and equal to that in bulk Ru metal. However, there are very substantial differences in the Ru–Ru coordination number between the two cases. These differences lie well outside the uncertainties estimated for the coordination numbers using the MAP routine in program EXCURVE (*5*) to investigate correlation between parameters (in this case between coordination number and Debye–Waller disorder). For the CeH_{2+x}/Ru and CeO_2/Ru catalysts, at the 95% level of confidence, these values are 5.3 ± 1.5 and 10.4 ± 1.8, respectively, taking into account the effect of using Fourier filtered first coordination shell data to carry out EXAFS modeling as discussed in Ref. (*9*). These differences are of course directly detectable in the experimental data by the large ($\times 2$) difference in EXAFS amplitudes (Figs. 3 and 5). We can therefore conclude that the active ammonia synthesis catalyst, which comprises cerium hydride and ruthenium particles, has a much smaller *average* Ru–Ru coordination number than does the inactive CeO_2/Ru system. In addition, a near-edge feature appears when the cerium hydride is oxidised to generate the inactive CeO_2/Ru catalyst.

Our X-ray diffraction studies under identical conditions (*3*) showed that the interaction of N_2/H_2 with $CeRu_2$ at 450°C results in the generation of material consisting of cerium hydride-supported ruthenium. Application of the Scherrer equation to the ruthenium peaks implied that the metal was present as 35-Å crystallites. *No change in the Scherrer-derived metal particle size was seen when the active cerium hydride-based catalyst was converted to the inactive cerium oxide-based catalyst.* However, very small crystallites (<20 Å) would not be detected by XRD, and indeed for particle sizes of ≤40 Å XAS is a much more powerful technique than XRD. Thus it seems likely that in the present case, the low average Ru–Ru coordination number observed in the CeH_{2+x}/Ru system is due to the presence of a large number of very small ruthenium clusters (as well as the XRD-visible ~35-Å particles); the low coordination numbers measured here strongly suggest the formation of very small ruthenium entities. Crystallite sizes may be estimated from the observed coordination numbers using published calculations for ideal cuboctahedral crystals (*10*) giving values of ~8 and 40 Å for the hydride- and oxide-supported systems, respectively. These sizes correspond to clusters containing ~13 and 1000 atoms, respectively. For the CeO_2/Ru system there is excellent agreement between the Ru particle sizes derived from XAS and XRD. Confirmation of the size of the Ru entities in at least this sample is given by examination of the Fourier transform radial distribution function derived from EXAFS. This shows a clear indication of higher coordination shells out to twice the first shell radius. The reduced relative contribution of these shells compared to those of bulk Ru is consistent with small particles and the measured increase in Debye–Waller disorder from EXCURVE. For example, for the first shell, the latter increases from a $2\sigma^2$ value of 0.009 for bulk metal to 0.014 ± 0.002 for CeO_2/Ru. For CeH_{2+x}/Ru, the higher shell contributions, if they exist, lie within the noise of the Fourier transform.

For the CeH_{2+x}/Ru catalyst where the coordination number is only 5.3 either a cluster of ~8 Å diameter containing only 13 atoms or a single layer raft of ruthenium ($n_c \lesssim 6$) could be postulated. However, XRD measurements taken under identical conditions show the presence of both cerium hydride *and* ruthenium. Figure 6 shows the XRD line profiles calculated from the Debye formula (*11*) for a 13-atom Ru cluster, a 20-Å raft, and a 30-Å Ru crystallite. These simulations show that only the latter could account for the major features of the Ru reflection. From a comparison of the simulated and observed XRD lineshapes it is clear that some of the ruthenium crystallites present are larger than 30 Å while others are smaller; i.e., a range of particle sizes exists. Nevertheless,

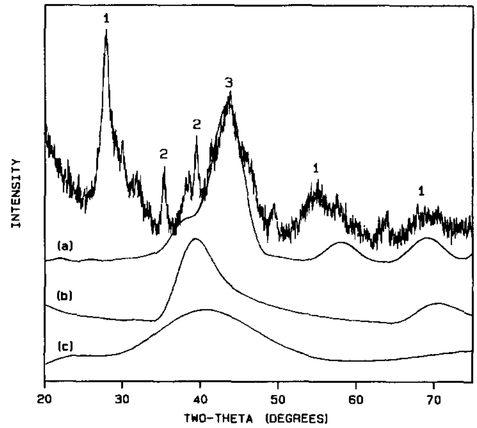

FIG. 6. XRD simulations overlaid on the raw CeH_{2+x}/Ru XRD data. The three simulations represent: (a) a 30-Å crystallite, (b) a 20-Å diameter raft, and (c) a 13-atom cluster. Peaks on the raw data correspond to: (1) CeH_{2+x}, (2) $CeRu_2H_x$, and (3) Ru.

within this range the coordination number for ruthenium in these crystallites will be ~10. As previously stated, it is very difficult to detect the presence of very small clusters by XRD so it is important to estimate the fraction of ruthenium found in these ~35-Å crystallites. This can be determined by quantitative analysis using a suitable internal standard. This has been done in two ways. First of all, the experimental ruthenium intensities were compared with those from a 2 : 1 molar mixture of crystalline CeO_2 and Ru under the same experimental conditions. A second and more reliable estimate can be obtained by noting that the XAS measurements imply that all of the Ru in the CeO_2/Ru catalyst exists as ~35 Å crystallites. This means that all of the Ru in the CeO_2/Ru sample is visible to the XRD technique, thereby providing an internal standard for the XRD measurements. From this we can deduce that ~60% of the Ru present in the CeH_{2+x}/Ru catalyst is visible in XRD. The same figure was obtained from the 2 : 1 molar mixture control experiment. This XRD-visible presence of 60% of the Ru in ~35-Å crystallites (n_c ~ 10) implies that the remaining ruthenium must have an ex-

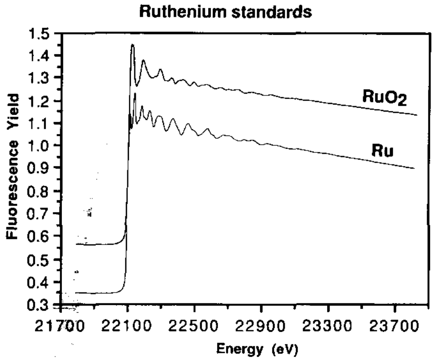

FIG. 7. XAS traces of the Ru and RuO_2 standard samples at room temperature. The vertical "Fluorescence Yield" scale applies only to the Ru data.

tremely low coordination number since the total average coordination number in the active CeH_{2+x}/Ru catalyst is 5.3. The average coordination number of the remaining Ru entities may well be less than 2. Since this material is associated with the cerium hydride the backscattering from the nearest-neighbour shell of hydrogen atoms would be too weak to be observed.

Thus a combination of XRD and XAS measurements leads to the conclusion that the ruthenium has a broad distribution of particle sizes. It is very clear, however, that a large number of Ru entities are extremely small, possibly comprising only one or two atoms. Somewhat ironically, the very small ruthenium particles are "invisible" to both XRD and EXAFS in the sense that in the former they do not contribute to the (102) reflection and in the latter the first coordination shell observed arises predominantly from the crystalline ruthenium particles.

In addition to a substantial increase in coordination number, oxidation of the hydride support also leads to the appearance of a near-edge feature in the XA spectra. Figure 7 shows XA spectra of Ru and RuO_2 standard samples. It can be seen that the near-edge feature is present in both traces, but it is distinctly more pronounced in the RuO_2 data. Such features, often referred to as "white lines," are caused by spectroscopic transitions ($\Delta l = \pm 1$) from 1*s* to unoccupied *p* states (*K*-edge) or 2*p* to unoccupied *d* states (L_2- and L_3-edges). Hence, L_2- and L_3-edge spectra can be used to probe *d*-band occupancy in transition metal systems, as demonstrated by the pioneering work of Lytle (*12*). In the cases of Au, Pt, Ir, and Ta, Lytle found an approximate correlation between the intensity of the white line feature and the estimated *d*-band occupancy, as determined from electron band structure calculations. The possibility of obtaining *d*-band character directly from white lines has stimulated many studies at the L_2 and L_3 absorption edges, especially in catalytic systems where correlations between electronic structure and chemical behaviour are sought (e.g., Refs. (*13–15*)).

Fewer studies have been carried out at the *K*-edge of transition metals, since these transitions do not directly probe the *d*-band. Theoretical studies have established that the white line observed in the *K*-edge structure of 4*d* transition metals such as Ru corresponds to transitions to the 5*p* band (*16, 17*). It should be stressed, however, that such calculations are not straightforward, since the spectral region being modeled lies between that most readily described by valence band calculations (pre-edge) and that described by multiple scattering (*18*). Nevertheless, our data show that these transitions are strongly suppressed in the CeH_{2+x}/Ru catalyst, so it is clear that the electronic structure of ruthenium in the hydride system is very different from that in the oxide. One possible explanation is that the suppression of these white line transitions in the hydride case is a direct result of electron transfer from the support to the ruthenium entities. This electronically modified ruthenium would then have a low 1*s*–5*p* transition probability and hence a white line feature of reduced intensity. In the CeO_2/Ru catalyst, on the other hand, any electron transfer would be expected to be in the opposite direction, i.e., from the ruthenium crystallites to the electronegative CeO_2 support, leading to an enhancement of the white line intensity. This is consistent with EXAFS data which indicate that in the Ru/Al_2O_3 and Ru/SiO_2 systems the metal is anchored to the support via Ru–O bonds (*19, 20*); it is also consistent with XPS results (*21*) which show that substantial charge transfer occurs from the metal phase in these systems. This interpretation is further supported by the XA spectra of the Ru and RuO_2 standards—the Ru species are expected to have a greater electron density in metallic Ru than in RuO_2, and the lowest white line intensity is in fact observed for Ru metal. The enhanced electron density hypothesis can also be invoked to explain the observed ammonia synthesis activity data. The rate-determining step in the reaction is believed to be the dissociation of the nitrogen molecule, with the atomic nitrogen undergoing subsequent hydrogenation on the metal surface (*22, 23*). The work of Ertl (*24*) on iron single crystals and that of Ozaki and co-workers (*25*) on ruthenium catalysts strongly suggests that the addition of alkali metal species, necessary in the generation of highly active conventional ammonia catalysts (*26*), promotes the reaction via electron transfer to the active catalytic site. This increase in the electron density of the active site facilitates the dissociative chemisorption of nitrogen by enhancing the back-donation from the metal orbitals to the antibonding π^* orbitals of the nitrogen molecule. This weakens the N–N bond, increases the rate of N_2 dissociation, and hence increases the rate of the reaction. In the CeH_{2+x}/Ru catalyst, the electron-rich Ru species should therefore have a high ammonia synthesis activity; correspondingly, the ruthenium in the CeO_2/Ru system has a lower electron density and exhibits much lower catalytic activity.

However, it is also possible that the observed near-edge behaviour is due entirely to the changes in particle size discussed above. Thus it is not necessarily correct to equate the number of p band vacancies with net electron vacancies. It is possible that an electron deficiency is not present at all, but that the number of observed p vacancies is made up by an increase in the number of d electrons via sp–d electron transfer. It is well known that the electronic structure of bulk metal atoms is different from that of isolated metal atoms. Metal atoms generally have more d character in the bulk metal; for example, atomic platinum has the configuration $5d^9 6s^1$ while bulk Pt adopts the configuration $5d^{9.7}6s^{0.3}$. It has been shown (*27, 28*) that the electronic rearrangement which occurs in bulk Ru is significantly smaller than this. The electronic structure of bulk Ru is $4d^{7.1}5s^{0.9}$, which compares with $4d^7 5s^1$ in atomic Ru. However, the possible effects of changes in particle size on the intensity of the white line feature should be considered here. Such a transfer of electrons from the bulk metal sp band to the d band would increase the $1s$-(sp) transition probability, leading to an increase in the intensity of the white line feature. Thus it is conceivable that the observed white line feature in the CeO_2/Ru system derives from what are essentially bulk metal atoms, while its absence in the CeH_{2+x}/Ru catalyst is indicative of a much lower average particle size, i.e., the atomic-like electronic properties. Indeed, the XAS spectra of the CeO_2/Ru catalyst and the Ru standard both exhibit the near-edge feature. The elucidation of electronic structure by analysis of K-edge spectra for second row transition metals is a relatively new technique, and most earlier publications concerned with supported, small metal particles have neither presented nor discussed experimental data. It is, therefore, difficult to separate support and size effects for any given metal. However, in the case of Ru, the electronic rearrangement which accompanies changes in metal dispersion is a relatively small effect: it therefore seems more likely that complete suppression of the white line feature in the CeH_{2+x}/Ru spectra is caused by *electron transfer from the hydride support to the Ru clusters*. In this connection, a recent theoretical calculation by Ravenek *et al.* (*29*) is of direct relevance. These authors have demonstrated the importance of final state effects in determining the intensity of white line features in XAS. Their principal conclusion was that in the absence of charge transfer effects small metal particles would be expected to give rise to a more intense white line feature than larger particles. In the present case, this strongly supports the view that the suppression of white line intensity in the case of the highly dispersed active catalyst is due to charge transfer from the support.

To summarise, observed differences in the EXAFS region of the spectra derived from CeH_{2+x}/Ru and CeO_2/Ru are due to changes in metal particle size. In the CeH_{2+x}/Ru system much of the ruthenium is present as very small particles; these very small particles have low Ru–Ru coordination numbers and exhibit no white line feature, due to charge transfer from the hydride support. When the support is oxidised the very small ruthenium entities grow rapidly and bulk Ru behaviour is observed, both in terms of the Ru–Ru coordination number *and* with the appearance of the white line feature. The higher activity of the CeH_{2+x}/Ru catalyst may then be a consequence of the much greater exposed Ru surface area in this system, although charge transfer from the electropositive support probably increases its activity further. Finally, it is also possible that hydrogen spillover to these electronically modified, highly dispersed ruthenium clusters occurs in the CeH_{2+x}/Ru catalyst.

CONCLUSIONS

1. Ruthenium metal is present in very different states in the two systems studied, CeH_{2+x}/Ru and CeO_2/Ru. The EXAFS and near-edge data imply that the inactive CeO_2/Ru catalyst contains essentially bulk ruthenium metal; on the other hand, in the catalytically active system CeH_{2+x}/Ru, the ruthenium appears to be present as a mixture of ~35-Å crystallites and very low coordination, electron-rich Ru clusters.

2. The activity of the CeH_{2+x}-based material appears to derive from an intimate interaction between the cerium hydride "support" and the highly dispersed transition metal clusters. This interaction may well be electronic in origin, although hydrogen spillover from the support phase is also a possibility.

ACKNOWLEDGMENTS

APW acknowledges financial support by the SERC and ICI plc under a CASE studentship. We are indebted to Dr. G. Owen for preparing the $CeRu_2$ samples and to Mr. G. Jenkins for assistance in interpreting the EXAFS data.

REFERENCES

1. Takeshita, T., Wallace, W. E., and Craig, R. S., *J. Catal.* **44,** 236 (1976).
2. Baglin, E. G., Atkinson, G. B., and Nicks, L. J., *Ind. Eng. Chem. Prod. Res. Dev.* **20,** 87 (1981).
3. Walker, A. P., Rayment, T., and Lambert, R. M., *J. Catal.* **117,** 102 (1989).
4. Nix, R. M., Rayment, T., Lambert, R. M., Jennings, J. R., and Owen, G., *J. Catal.* **106,** 216 (1987).
5. Gurman, S. J., Binsted, N., and Ross, I., *J. Phys. C* **17,** 143 (1984).
6. Jaklevic, J., Kirby, J. A., Klein, M. P., Robertson, A. S., Brown, G. S., and Eisenburger, P., *Solid State Comm.* **23,** 679 (1977).
7. Jones, S., and Oldman, R. J., unpublished work.
8. Tan, Z., Budnick, J. I., and Heald, S. M., *Rev. Sci. Instrum.* **60,** 1021 (1989).
9. Joyner, R. W., Martin, K. H., and Meehan, P., *J. Phys. C.* **20,** 4005 (1987).
10. Chini, P., *Gazz. Chim. Ital.* **109,** 225 (1979).
11. Guinier, A., "X-ray Diffraction," p. 48. Freeman, San Francisco, 1963.
12. Lytle, F. W., *J. Catal.* **43,** 376 (1976).
13. Lytle, F. W., Wei, P. S. P., Greegor, R. B., Via, G. H., and Sinfelt, J. H., *J. Chem. Phys.* **70,** 4849 (1979).
14. Horsley, J. A., *J. Chem. Phys.* **76,** 1451 (1982).
15. De Crescenzi, M., Diociaiuti, M., Picozzi, P., and Santucci, S., *Phys. Rev. B* **34,** 4334 (1986).
16. Kostroun, V. O., Fairchild, R. W., Kukkonen, C. A., and Wilkins, J. W., *Phys. Rev. B* **13,** 3268 (1976).
17. Muller, J. E., Jepsen, O., Andersen, O. K., and Wilkins, J. W., *Phys. Rev. Lett.* **40,** 720 (1978).
18. Bianconi, A., EXAFS for Inorganic Systems, p. 13. Proc. Daresbury Study Weekend, SERC, 1981.
19. Vlaic, G., Bart, J. C. J., Cavigiolo, W., Furesi, A., Ragaini, V., Cattania Sabbadini, M. G., and Burattini, E., *J. Catal.* **107,** 263 (1987).
20. Lytle, F. W., Via, G. H., and Sinfelt, J. H., *J. Chem. Phys.* **67,** 3831 (1977).
21. Bossi, A., Garbassi, F., and Petrini, G., *J. Chem. Soc. Faraday Trans. 1* **78,** 1029 (1982).

22. Bokhoven, C., Gorgels, M. J., and Mars, P., *Trans. Faraday Soc.* **55,** 315 (1959).
23. Yamamoto, O., Tanaka, S., and Tanaka, K., *Sci. Pap. Inst. Phys. Chem. Res.* **68,** 8 (1974).
24. Ertl, G., Lee, S. B., and Weiss, M., *Surf. Sci.* **114,** 527 (1982).
25. Aika, K. I., Hori, H., and Ozaki, A., *J. Catal.* **27,** 424 (1972).
26. Mittasch, A., *in* "Advances in Catalysis" (W. G. Frankenberg, V. I. Komarewsky, and E. K. Rideal, Eds.), Vol. 2, p. 81. Academic Press, New York, 1950.
27. Jepsen, O., Krogh Andersen, O., and Mackintosh, A. R., *Phys. Rev. B* **12,** 3084 (1975).
28. Baetzold, R. C., *Inorg. Chem.* **20,** 118 (1981).
29. Ravenek, W., Jansen, A. P. J., and van Santen, R. A., *J. Phys. Chem.* **93,** 6445 (1989).